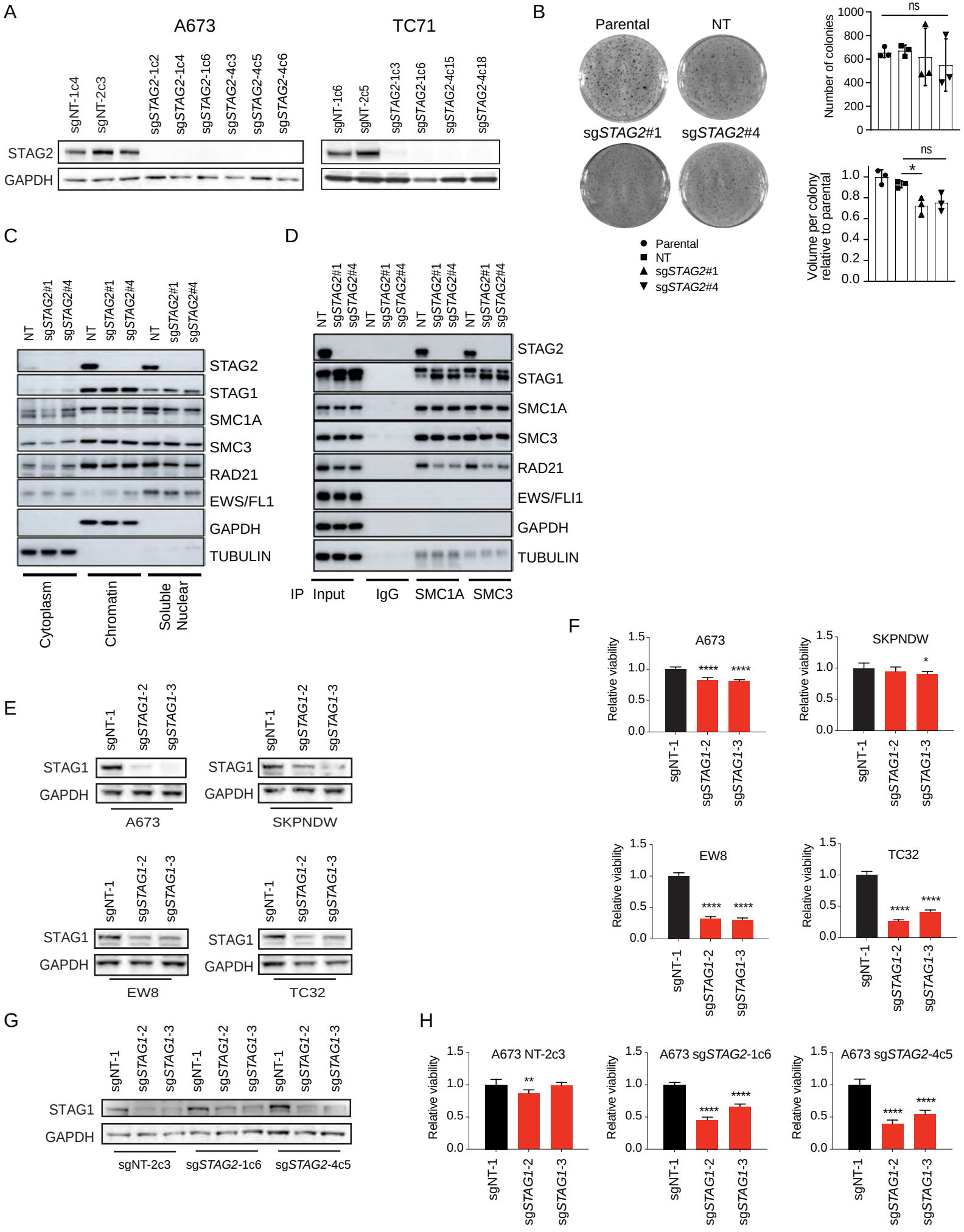
A
A673
TC71
sgNT-1c4
sgNT-2c3
sgSTAG2-1c2
sgSTAG2-1c4
sgSTAG2-1c6
sgSTAG2-4c3
sgSTAG2-4c5
sgSTAG2-4c6
sgNT-1c6
sgNT-2c5
sgSTAG2-1c3
sgSTAG2-1c6
sgSTAG2-4c15
sgSTAG2-4c18
STAG2
GAPDH
B
Parental
NT
sgSTAG2#1
sgSTAG2#4
Parental
NT
sgSTAG2#1
sgSTAG2#4
Number of colonies
ns
Volume per colony relative to parental
ns
*
C
NT
sgSTAG2#1
sgSTAG2#4
STAG2
STAG1
SMC1A
SMC3
RAD21
EWS/FL1
GAPDH
TUBULIN
Cytoplasm
Chromatin
Soluble Nuclear
D
NT
sgSTAG2#1
sgSTAG2#4
STAG2
STAG1
SMC1A
SMC3
RAD21
EWS/FLI1
GAPDH
TUBULIN
IP
Input
IgG
SMC1A
SMC3
E
sgNT-1
sgSTAG1-2
sgSTAG1-3
STAG1
GAPDH
A673
SKPNDW
EW8
TC32
F
A673
SKPNDW
EW8
TC32
Relative viability
sgNT-1
sgSTAG1-2
sgSTAG1-3
G
sgNT-1
sgSTAG1-2
sgSTAG1-3
STAG1
GAPDH
sgNT-2c3
sgSTAG2-1c6
sgSTAG2-4c5
H
A673 NT-2c3
A673 sgSTAG2-1c6
A673 sgSTAG2-4c5
Relative viability
sgNT-1
sgSTAG1-2
sgSTAG1-3

Figure S1. Loss of *STAG2* does not dramatically alter cell proliferation but changes the composition of the cohesin complex and renders cells sensitive to *STAG1* deletion, related to Figure 1.

(A) Western blot showing the expression levels of *STAG2* in clonally selected A673 (left) and TC71 (right). GAPDH is used as a loading control.

(B) TC71 cells were plated in methylcellulose media for 14 days. Shown are mean ± standard deviation barplots for the number of colonies (top) and for the volume per colony relative to parental (bottom). One-way ANOVA Tukey's multiple comparisons test, ns = not significant, * $P < 0.05$.

(C) Cell fractionation followed by western blot was performed on the lysates from the indicated cellular compartments in clonally selected control and *STAG2* KO TC71 cells.

(D) Immunoprecipitation was performed on whole cell lysates using bead conjugated antibodies against either SMC1A, SMC3 or IgG in control and *STAG2* KO TC71 cells. Total proteins pulled down with the antibodies were recovered and immunoblotted for the indicated proteins.

(E) Polyclonal *STAG1* KO cells were generated via CRISPR/Cas9 mediated editing in two *STAG2* WT (A673 & SKPNDW) and STAG2 mutant (TC32 & EW8) Ewing cell lines. Western blot shows the levels of STAG1 in each cell line. GAPDH is used as a loading control.

(F) Short-term cell viability assays were performed using CellTiter-Glo in control and *STAG1* KO cells described in Figure S1E. Bar graphs represent mean and standard deviation, Student t-test, * $P < 0.05$, **** $P < 0.0001$.

(G) Polyclonal *STAG1* KO cells were generated via CRISPR/Cas9 mediated editing in clonally selected control (NT) and two independent *STAG2* KO A673 cells. Western blot shows the levels of STAG1 in each cell line. GAPDH is used as a loading control.

(H) Short-term cell proliferation assays were performed using CellTiter-Glo in control and *STAG1* KO cells described in Figure S1G. Bar graphs represent mean and standard deviation, Student t-test, ** $P < 0.01$, **** $P < 0.0001$.

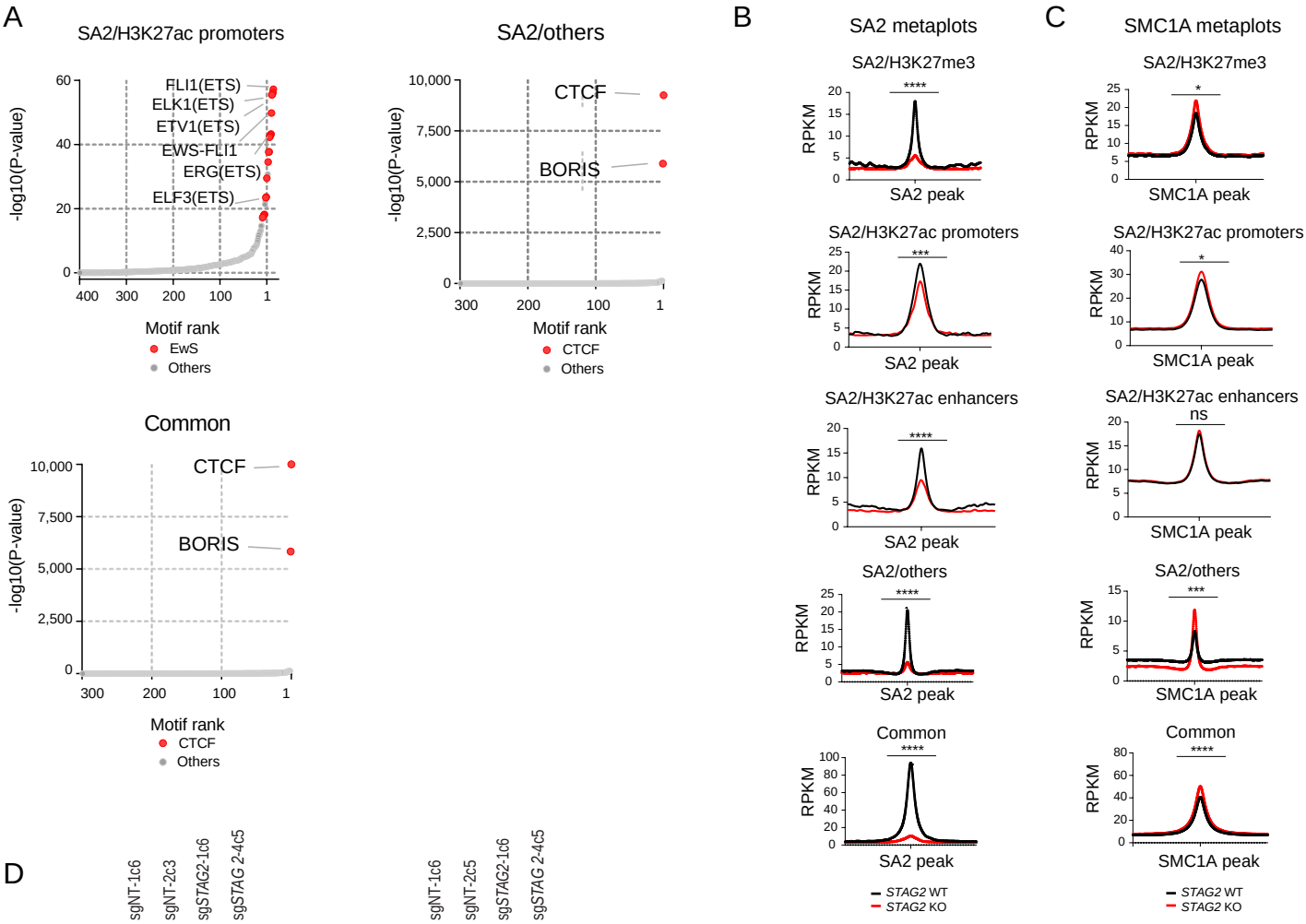
A
SA2/H3K27ac promoters
-log10(P-value)
FLI1(ETS)
ELK1(ETS)
ETV1(ETS)
EWS-FLI1
ERG(ETS)
ELF3(ETS)
Motif rank
EwS
Others
SA2/others
CTCF
BORIS
CTCF
Others
Common
CTCF
BORIS
CTCF
Others
B
SA2 metaplots
SA2/H3K27me3
SA2/H3K27ac promoters
SA2/H3K27ac enhancers
SA2/others
Common
RPKM
SA2 peak
C
SMC1A metaplots
SA2/H3K27me3
SA2/H3K27ac promoters
SA2/H3K27ac enhancers
ns
SA2/others
Common
SMC1A peak
STAG2 WT
STAG2 KO
D
sgNT-1c6
sgNT-2c3
sgSTAG2-1c6
sgSTAG 2-4c5
STAG2
EWS/FLI1
GAPDH
A673
sgNT-1c6
sgNT-2c5
sgSTAG2-1c6
sgSTAG 2-4c5
STAG2
EWS/FLI1
GAPDH
TC71
E
EWS/FLI1
WT
KO
Genome-wide binding sites (25,220)
-5 kb
5 kb
F
EWS/FLI1 metaplot
RPKM
EWS/FLI1 peak
STAG2 WT
STAG2 KO

Figure S2. *STAG2* is enriched at PRC2 and enhancer marked regions and its deletion is incompletely compensated by *STAG1*, related to Figure 2.

(A) Hockey plots depicting motifs enriched in SA2/H3K27ac promoters, SA2/others and Common regions defined in Figure 2C.

(B)-(C) Metaplots showing average peak centered signal for (B) SA2 and (C) SMC1A in the cohesin regions defined in Figure 2C. Differential read density in *STAG2* KO vs. WT A673 cells based on unpaired t-test with Welch's correction, **** $P < 0.0001$, *** $P < 0.001$, * $P < 0.05$, ns = not significant.

(D) Western blot showing the expression levels of EWS/FLI1 in clonally selected control and *STAG2* KO A673 (left) and TC71 (right). GAPDH is used as a loading control.

(E) Genome-wide heatmap depicting EWS/FLI1 peak centered signal in control and *STAG2* KO A673 cells.

(F) Metaplot showing genome-wide average peak centered read density of EWS/FLI1 signal in control and *STAG2* KO A673 cells. Differential read density in KO vs. WT conditions based on unpaired t-test with Welch's correction, * $P < 0.05$.

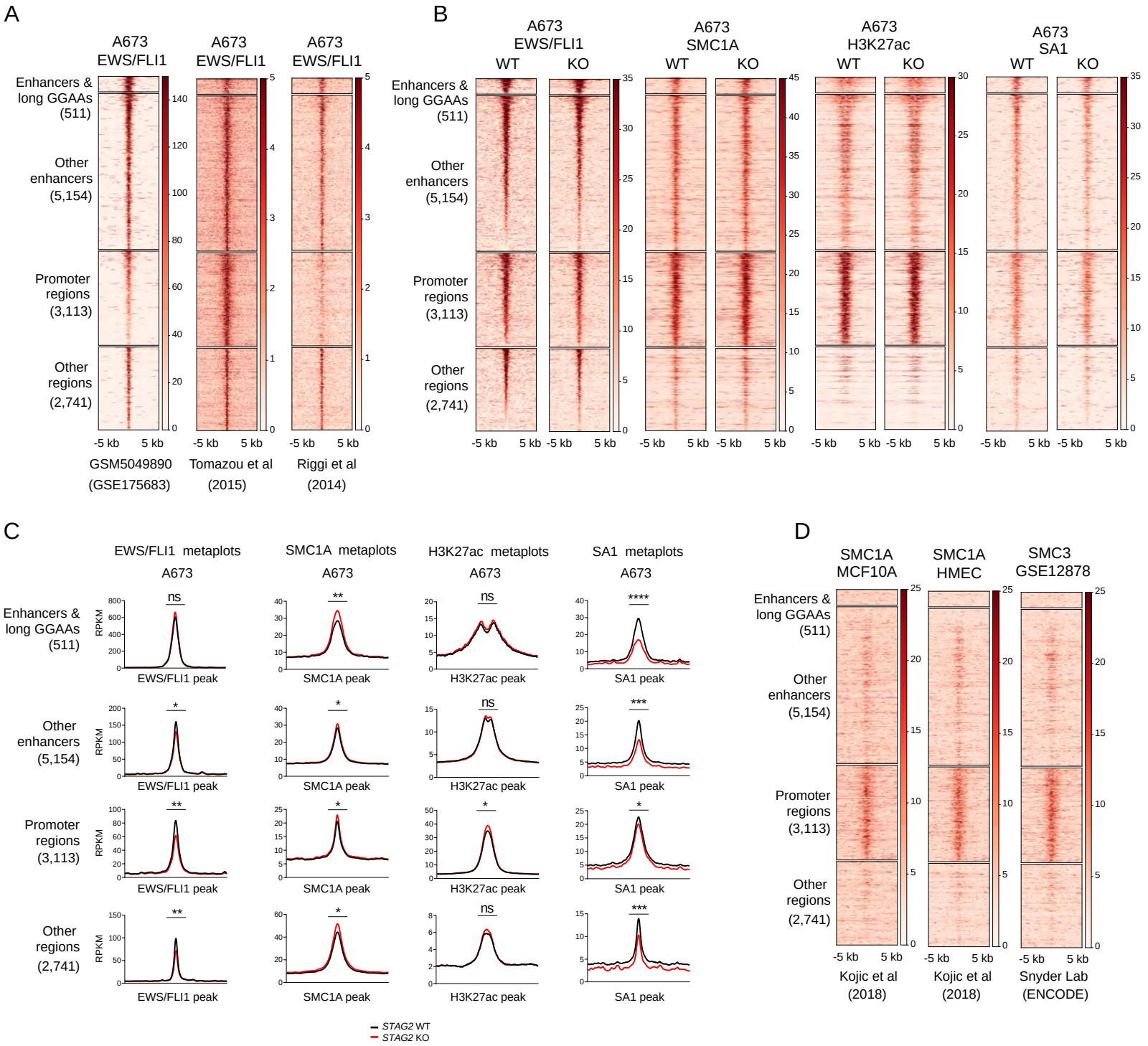
A
A673 EWS/FLI1
A673 EWS/FLI1
A673 EWS/FLI1
Enhancers & long GGAAs (511)
Other enhancers (5,154)
Promoter regions (3,113)
Other regions (2,741)
-5 kb
5 kb
GSM5049890 (GSE175683)
Tomazou et al (2015)
Riggi et al (2014)
B
A673 EWS/FLI1
A673 SMC1A
A673 H3K27ac
A673 SA1
WT
KO
C
EWS/FLI1 metaplots
SMC1A metaplots
H3K27ac metaplots
SA1 metaplots
A673
RPKM
EWS/FLI1 peak
SMC1A peak
H3K27ac peak
SA1 peak
STAG2 WT
STAG2 KO
D
SMC1A MCF10A
SMC1A HMEC
SMC3 GSE12878
Kojic et al (2018)
Kojic et al (2018)
Snyder Lab (ENCODE)
E
EWS/FLI1 differential loops
loop length (kb)
Decreased
Increased

Figure S3. Loss of *STAG2* alters the frequency of cis-chromatin contacts, related to Figure 3.

(A) Heatmaps depicting the EWS/FLI1 binding on the high confidence EWS/FLI1 consensus peaks generated from the intersection of 3 independent studies, all in A673 cells: this current study (GEO: GSM5049890), (Riggi et al., 2014; Tomazou et al., 2015) and presented in Table S1**.** Heatmaps are clustered in four regions defined by EWS/FLI1 peaks in (*i*) H3K27ac enhancers with long (≥4) GGAA repeats; (*ii*) other H3K27ac enhancers (with no long GGAA repeats); (*iii*) TSS+/-3kb promoter regions; (*iv*) other regions.

(B) EWS/FLI1, SMC1A, and H3K27ac in WT and *STAG2* KO signal in A673 cells on the clusters of high confidence EWS/FLI1 consensus peaks shown in Figure S3A.

(C) Read density metaplots showing average RPKM normalized signal for EWS/FLI1, SMC1A, H3K27ac and SA1 in WT (black) and *STAG2* KO (red) A673 cells. Differential read density in KO vs. WT conditions, unpaired t-test with Welch's correction, **** $P < 0.0001$, ns = not significant.

(D) Clustered heatmaps showing cohesin binding in non-Ewing sarcoma cells in the EWS/FLI1 regions defined in Figure S3A: SMC1A in MCF10 and HMEC cells (Kojic et al., 2018) and SMC3 in GM12878 cells (ENCODE, Snyder Lab).

(E) Median with 95% confidence interval plots for lengths of EWS/FLI1 differential loops with decreased vs. increased contact coverage in *STAG2* KO vs. WT A673 cells. Unpaired t-test with Welch correction, **** $P < 0.0001$.

Table S2. Top 30 motifs enriched in enhancers involved in the differential Enhancer-Promoter interactions, related to Figure 3.

#	Motif name	Consensus sequence	-log10(P-value)
1	Bach2(bZIP)/OCILy7-Bach2-ChIP-Seq(GSE44420)	TGCTGAGTCA	1.20E+01
2	Jun-AP1(bZIP)/K562-cJun-ChIP-Seq(GSE31477)	GATGASTCATCN	1.16E+01
3	Nrf2(bZIP)/Lymphoblast-Nrf2-ChIP-Seq(GSE37589)	HTGCTGAGTCAT	1.07E+01
4	Bach1(bZIP)/K562-Bach1-ChIP-Seq(GSE31477)	AWWNTGCTGAGTCAT	1.06E+01
5	Fosl2(bZIP)/3T3L1-Fosl2-ChIP-Seq(GSE56872)	NATGASTCABNN	9.54E+00
6	CTCF-SatelliteElement(Zf?)/CD4+-CTCF-ChIP-Seq(Barski_et_al.)	TGCAGTTCCMVNWRTGGCCA	8.84E+00
7	EWS:FLI1-fusion(ETS)/SK_N_MC-EWS:FLI1-ChIP-Seq(SRA014231)	VACAGGAAAT	8.10E+00
8	Ets1-distal(ETS)/CD4+-PolII-ChIP-Seq(Barski_et_al.)	MACAGGAAGT	7.73E+00
9	NF-E2(bZIP)/K562-NFE2-ChIP-Seq(GSE31477)	GATGACTCAGCA	6.90E+00
10	ERG(ETS)/VCaP-ERG-ChIP-Seq(GSE14097)	ACAGGAAGTG	6.89E+00
11	JunB(bZIP)/DendriticCells-Junb-ChIP-Seq(GSE36099)	RATGASTCAT	6.72E+00
12	Rfx6(HTH)/Min6b1-Rfx6.HA-ChIP-Seq(GSE62844)	TGTTKCCTAGCAACM	6.22E+00
13	GABPA(ETS)/Jurkat-GABPa-ChIP-Seq(GSE17954)	RACCGGAAGT	6.11E+00
14	PAX5(Paired,Homeobox)/GM12878-PAX5-ChIP-Seq(GSE32465)	GCAGCCAAGCRTGACH	6.11E+00
15	Atf3(bZIP)/GBM-ATF3-ChIP-Seq(GSE33912)	DATGASTCATHN	6.00E+00
16	BATF(bZIP)/Th17-BATF-ChIP-Seq(GSE39756)	DATGASTCAT	5.93E+00
17	CEBP:AP1(bZIP)/ThioMac-CEBPb-ChIP-Seq(GSE21512)	DRTGTTGCAA	5.91E+00
18	Fra2(bZIP)/Striatum-Fra2-ChIP-Seq(GSE43429)	GGATGACTCATC	5.86E+00
19	Fra1(bZIP)/BT549-Fra1-ChIP-Seq(GSE46166)	NNATGASTCATH	5.84E+00
20	EWS:ERG-fusion(ETS)/CADO_ES1-EWS:ERG-ChIP-Seq(SRA014231)	ATTTCCTGTN	5.79E+00
21	TEAD4(TEA)/Tropoblast-Tead4-ChIP-Seq(GSE37350)	CCWGGAATGY	5.41E+00
22	ELF5(ETS)/T47D-ELF5-ChIP-Seq(GSE30407)	ACVAGGAAGT	4.87E+00
23	ETV1(ETS)/GIST48-ETV1-ChIP-Seq(GSE22441)	AACCGGAAGT	4.85E+00
24	AP-1(bZIP)/ThioMac-PU.1-ChIP-Seq(GSE21512)	VTGACTCATC	4.70E+00
25	GATA(Zf),IR4/iTreg-Gata3-ChIP-Seq(GSE20898)	NAGATWNBNATCTNN	4.68E+00
26	MafK(bZIP)/C2C12-MafK-ChIP-Seq(GSE36030)	GCTGASTCAGCA	4.62E+00
27	EHF(ETS)/LoVo-EHF-ChIP-Seq(GSE49402)	AVCAGGAAGT	4.55E+00
28	ZNF322(Zf)/HEK293-ZNF322.GFP-ChIP-Seq(GSE58341)	GAGCCTGGTACTGWGCCTGR	4.38E+00
29	Chop(bZIP)/MEF-Chop-ChIP-Seq(GSE35681)	ATTGCATCAT	4.32E+00
30	CArG(MADS)/PUER-Srf-ChIP-Seq(Sullivan_et_al.)	CCATATATGGNM	4.23E+00

* Significance P-value < 0.0001 estimated by Homer v4.11. ETS and EWS/FLI1 motifs are highlighted yellow.

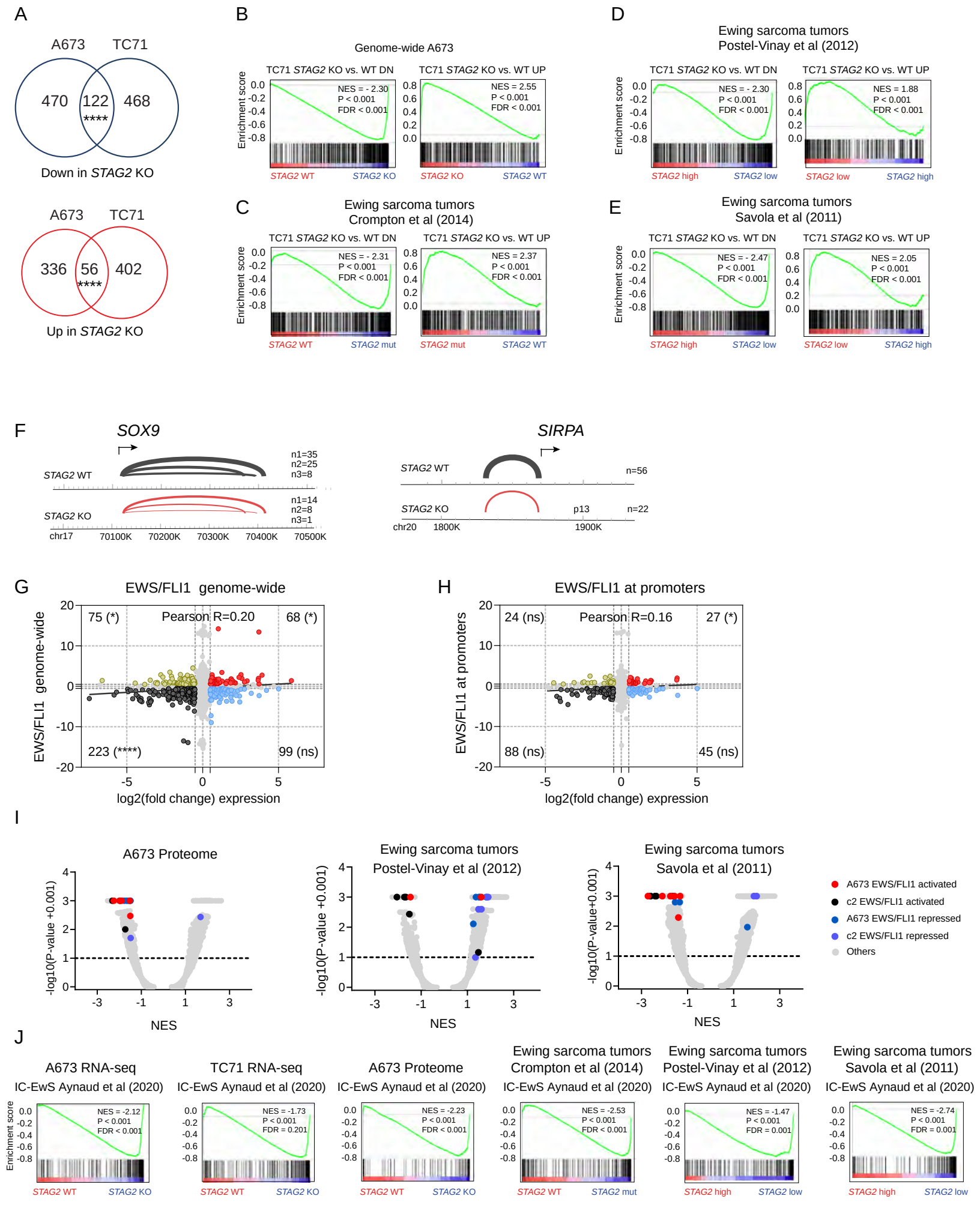
A
A673
TC71
470
122
468
****
Down in STAG2 KO
A673
TC71
336
56
402
****
Up in STAG2 KO
B
Genome-wide A673
TC71 STAG2 KO vs. WT DN
NES = - 2.30
P < 0.001
FDR < 0.001
TC71 STAG2 KO vs. WT UP
NES = 2.55
P < 0.001
FDR < 0.001
Enrichment score
STAG2 WT
STAG2 KO
STAG2 KO
STAG2 WT
C
Ewing sarcoma tumors
Crompton et al (2014)
TC71 STAG2 KO vs. WT DN
NES = - 2.31
P < 0.001
FDR < 0.001
TC71 STAG2 KO vs. WT UP
NES = 2.37
P < 0.001
FDR < 0.001
STAG2 WT
STAG2 mut
STAG2 mut
STAG2 WT
D
Ewing sarcoma tumors
Postel-Vinay et al (2012)
TC71 STAG2 KO vs. WT DN
NES = - 2.30
P < 0.001
FDR < 0.001
TC71 STAG2 KO vs. WT UP
NES = 1.88
P < 0.001
FDR < 0.001
STAG2 high
STAG2 low
STAG2 low
STAG2 high
E
Ewing sarcoma tumors
Savola et al (2011)
TC71 STAG2 KO vs. WT DN
NES = - 2.47
P < 0.001
FDR < 0.001
TC71 STAG2 KO vs. WT UP
NES = 2.05
P < 0.001
FDR < 0.001
STAG2 high
STAG2 low
STAG2 low
STAG2 high
F
SOX9
STAG2 WT
n1=35
n2=25
n3=8
STAG2 KO
n1=14
n2=8
n3=1
chr17
70100K
70200K
70300K
70400K
70500K
SIRPA
STAG2 WT
n=56
STAG2 KO
p13
n=22
chr20
1800K
1900K
G
EWS/FLI1 genome-wide
75 (*)
Pearson R=0.20
68 (*)
223 (****)
99 (ns)
EWS/FLI1 genome-wide
log2(fold change) expression
H
EWS/FLI1 at promoters
24 (ns)
Pearson R=0.16
27 (*)
88 (ns)
45 (ns)
EWS/FLI1 at promoters
log2(fold change) expression
I
A673 Proteome
Ewing sarcoma tumors
Postel-Vinay et al (2012)
Ewing sarcoma tumors
Savola et al (2011)
-log10(P-value +0.001)
NES
A673 EWS/FLI1 activated
c2 EWS/FLI1 activated
A673 EWS/FLI1 repressed
c2 EWS/FLI1 repressed
Others
J
A673 RNA-seq
IC-EwS Aynaud et al (2020)
NES = -2.12
P < 0.001
FDR < 0.001
STAG2 WT
STAG2 KO
TC71 RNA-seq
IC-EwS Aynaud et al (2020)
NES = -1.73
P < 0.001
FDR = 0.201
STAG2 WT
STAG2 KO
A673 Proteome
IC-EwS Aynaud et al (2020)
NES = -2.23
P < 0.001
FDR < 0.001
STAG2 WT
STAG2 KO
Ewing sarcoma tumors
Crompton et al (2014)
IC-EwS Aynaud et al (2020)
NES = -2.53
P < 0.001
FDR < 0.001
STAG2 WT
STAG2 mut
Ewing sarcoma tumors
Postel-Vinay et al (2012)
IC-EwS Aynaud et al (2020)
NES = -1.47
P < 0.001
FDR = 0.001
STAG2 high
STAG2 low
Ewing sarcoma tumors
Savola et al (2011)
IC-EwS Aynaud et al (2020)
NES = -2.74
P < 0.001
FDR = 0.001
STAG2 high
STAG2 low
Enrichment score

Figure S4. Loss of *STAG2* alters the EWS/FLI1 driven oncogenic transcriptional program, related to Figure 4.

(A) Venn diagram showing the overlap between down-regulated and up-regulated differentially expressed genes (|log2(fold change)| ≥ 1.5, adjusted P ≤ 0.10) in *STAG2* KO vs. *STAG2* WT A673 and TC71 cells. Two-tailed Fisher exact test, **** P < 0.0001.

(B)-(E) GSEA plots demonstrating the enrichment of the *STAG2* KO vs. WT gene signature in TC71 cells (|log2(fold change)| ≥ 1.5, adjusted P ≤ 0.10) in (B) genome-wide mRNA expression signature of *STAG2* KO vs. *STAG2* WT in A673 cells (C) *STAG2* mutant vs. *STAG2* WT primary Ewing sarcoma tumors (Crompton et al., 2014) and *STAG2* low expression vs. *STAG2* high expression tumors in primary Ewing sarcoma tumors (D) (Postel-Vinay et al., 2012) and (E) (Savola et al., 2011).

(F) Diagrams showing the EWS/FLI1 differential loop structures (long interaction arcs connecting anchored regions) at the *SOX9* locus on chromosome 17 and at the *SIRPA* locus on chromosome 20 in WT (black) and *STAG2* KO (red) A673 cells. Numbers on the right show the contact read coverage at loop anchors. Diagrams were created on the WashU Epigenome Browser platform.

(G) Scatter plot depicting the overlap between the 5,192 genes with significant changes induced by *STAG2* KO in A673 cells for EWS/FLI1 ChIP-Seq genome-wide binding (abs(Delta area under curve signal) ≥ 1.5): decreased (3,714 genes) or increased (1,478 genes) vs. the 984 genes with significant expression changes (|log2(fold change)| ≥ 1.5, adjusted P ≤ 0.10): down-regulated (592 genes), up-regulated (392 genes). Two-tailed Fisher exact test, **** P < 0.0001, * P < 0.05, ns = not significant.

(H) Scatter plot depicting the overlap between the 2,640 genes with EWS/FLI1 ChIP-Seq promoter binding changes induced by *STAG2* KO in A673 cells (abs(Delta for area under curve signal) ≥ 1.5): decreased (2,008 genes) or increased (632 genes) vs. the 984 genes with significant expression changes (|log2(fold change)| ≥ 1.5, adjusted P ≤ 0.1): down-regulated (592

genes), up-regulated (392 genes). Two-tailed Fisher exact test, **** P < 0.0001, * P < 0.05, ns = not significant.

(I) Volcano plots depicting gene set enrichment analyses for the proteomic expression changes induced by *STAG2* KO vs. WT on A673 cells (left) and *STAG2* low vs *STAG2* high expression in two Ewing tumor expression data sets vs. the union of a collection of 12 EWS/FLI1 gene signatures on A673 cells from published data and MSigDB v7.1 c2 collection (5,529 gene sets). Activated EWS/FLI1 gene signatures are highlighted in red (12 EWS/FLI1 gene sets, compendia collection) and in black (MSigDB c2). Repressed EWS/FLI1 signatures are highlighted in blue (12 EWS/FLI gene sets, compendia collection) and in purple (MSigDB c2).

(J) GSEA plots showing enrichment of the recently generated A673 Ewing sarcoma gene signature IC-EwS (Aynaud et al., 2020) for *STAG2* KO vs. WT in A673 (RNA-Seq and Proteome) and TC71 (RNA-Seq) data, *STAG2* mutant vs *STAG2* WT tumor samples from (Crompton et al., 2014) and *STAG2* low vs. *STAG2* high expression tumor samples from Postel-Vinay et al. (2012) and Savola et al. (2019). Normalized enrichment, P-value and FDR scores are indicated in each plot.

A

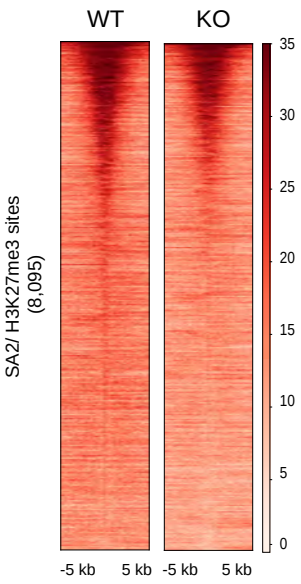
H3K27me3 at SA2/H3K27me3 sites
WT
KO
SA2/ H3K27me3 sites
(8,095)
35
30
25
20
15
10
5
0
-5 kb
5 kb
-5 kb
5 kb

B

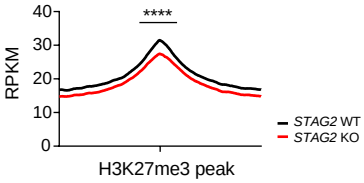
H3K27me3 metaplot
****
RPKM
40
30
20
10
0
STAG2 WT
STAG2 KO
H3K27me3 peak

C

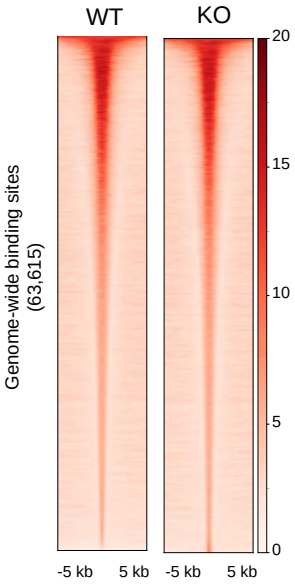
H3K27ac genome-wide
WT
KO
Genome-wide binding sites
(63,615)
20
15
10
5
0
-5 kb
5 kb
-5 kb
5 kb

D

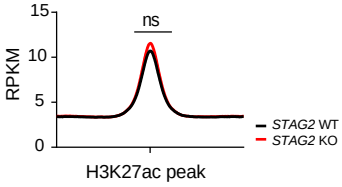
H3K27ac metaplot
ns
RPKM
15
10
5
0
STAG2 WT
STAG2 KO
H3K27ac peak

E

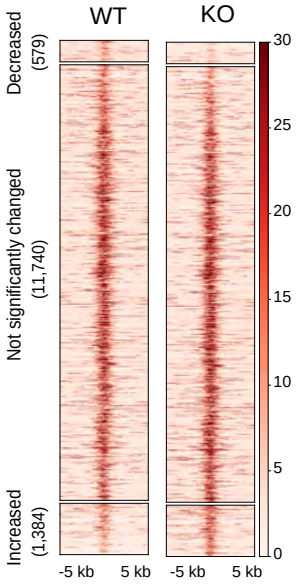
H3K27ac at promoters
WT
KO
Decreased
(579)
Not significantly changed
(11,740)
Increased
(1,384)
30
25
20
15
10
5
0
-5 kb
5 kb
-5 kb
5 kb

F

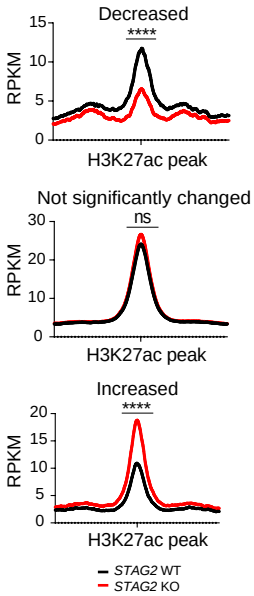
H3K27ac metaplots
Decreased
****
RPKM
15
10
5
0
H3K27ac peak
Not significantly changed
ns
RPKM
30
20
10
0
H3K27ac peak
Increased
****
RPKM
20
15
10
5
0
H3K27ac peak
STAG2 WT
STAG2 KO

G

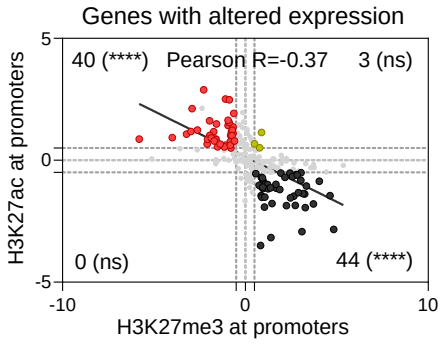
Genes with altered expression
40 (****)
Pearson R=-0.37
3 (ns)
0 (ns)
44 (****)
H3K27ac at promoters
H3K27me3 at promoters
5
0
-5
-10
0
10

Figure S5. Loss of *STAG2* perturbs PRC2 mediated regulation of gene expression, related to Figure 5.

(A) Genome-wide heatmap depicting H3K27me3 signal intensities at the cohesin SA2/H3K27me3 regions defined in Figure 2C in control and *STAG2* KO A673 cells.

(B) Metaplot showing average read density of H3K27me3 signal in *STAG2* WT and KO conditions on A673 cells around peak centered regions defined in Figure S5A. Unpaired t-test with Welch's correction, * $P < 0.05$.

(C) Genome-wide heatmaps of H3K27ac ChIP-Seq signal in A673 cells expressing *STAG2* WT (left) or *STAG2* KO (right) centered on peaks identified in either or both conditions.

(D) Metaplots showing average genome-wide H3K27ac signal in *STAG2* KO and WT A673 cells. Differential read density, unpaired t-test with Welch's correction, **** $P < 0.0001$.

(E) Clustered heatmaps depicting TSS +/- 5kb promoter regions with decreased, not significantly changed, or increased H3K27ac ChIP-Seq signal in *STAG2* KO vs. WT A673 cells (abs(Delta area under curve signal) ≥ 1.5).

(F) Metaplots showing average H3K27ac signal in the promoter regions defined in Figure 5D.

(G) Scatter plot for the synergistic changes of H3K27me3 vs. H3K27ac ChIP-Seq binding signal at the promoter regions in the universe of differentially expressed genes in *STAG2* KO vs. WT A673 cells. Two-tailed Fisher exact test, **** $P < 0.0001$, ns = not significant.

Table S6. Top 30 enriched motifs for the promoters of genes with significantly altered H3K27me3 binding levels induced by *STAG2* KO vs. WT in A673 cells, related to Figure 5.

#	Motif Name	Consensus	-log10(P-value)
1	Pdx1(Homeobox)/Islet-Pdx1-ChIP-Seq(SRA008281)	YCATYAATCA	9.91E+00
2	PBX2(Homeobox)/K562-PBX2-ChIP-Seq(Encode)	RTGATTKATRGN	6.84E+00
3	Pit1+1bp(Homeobox)/GCrat-Pit1-ChIP-Seq(GSE58009)	ATGCATAATTCA	6.17E+00
4	EBF2(EBF)/BrownAdipose-EBF2-ChIP-Seq(GSE97114)	NABTCCCWDGGGAVH	6.10E+00
5	AR-halfsite(NR)/LNCaP-AR-ChIP-Seq(GSE27824)	CCAGGAACAG	6.02E+00
6	EBF(EBF)/proBcell-EBF-ChIP-Seq(GSE21978)	DGTCCCYRGGGA	5.20E+00
7	HOXB13(Homeobox)/ProstateTumor-HOXB13-ChIP-Seq(GSE56288)	TTTTATKRGG	5.16E+00
8	EWS:ERG-fusion(ETS)/CADO_ES1-EWS:ERG-ChIP-Seq(SRA014231)	ATTTCCTGTN	4.91E+00
9	Oct2(POU,Homeobox)/Bcell-Oct2-ChIP-Seq(GSE21512)	ATATGCAAAT	4.89E+00
10	HOXA1(Homeobox)/mES-Hoxa1-ChIP-Seq(SRP084292)	TGATKGATGR	4.89E+00
11	HOXA2(Homeobox)/mES-Hoxa2-ChIP-Seq(Donaldson_et_al.)	GYCATCMATCAT	4.85E+00
12	FOXM1(Forkhead)/MCF7-FOXM1-ChIP-Seq(GSE72977)	TRTTTACTTW	4.50E+00
13	NFAT(RHD)/Jurkat-NFATC1-ChIP-Seq(Jolma_et_al.)	ATTTTCCATT	4.45E+00
14	Pbx3(Homeobox)/GM12878-PBX3-ChIP-Seq(GSE32465)	SCTGTCAMTCAN	4.38E+00
15	CUX1(Homeobox)/K562-CUX1-ChIP-Seq(GSE92882)	TATCGATNAN	4.16E+00
16	Oct6(POU,Homeobox)/NPC-Pou3f1-ChIP-Seq(GSE35496)	WATGCAAATGAG	3.97E+00
17	Hoxa13(Homeobox)/ChickenMSG-Hoxa13.Flag-ChIP-Seq(GSE86088)	CYHATAAAAN	3.95E+00
18	Atf4(bZIP)/MEF-Atf4-ChIP-Seq(GSE35681)	MTGATGCAAT	3.93E+00
19	SCL(bHLH)/HPC7-Scl-ChIP-Seq(GSE13511)	AVCAGCTG	3.87E+00
20	ZNF652/HepG2-ZNF652.Flag-ChIP-Seq(Encode)	TTAACCCTTTVNKKN	3.86E+00
21	Pax7(Paired,Homeobox),long/Myoblast-Pax7-ChIP-Seq(GSE25064)	TAATCHGATTAC	3.62E+00
22	PBX1(Homeobox)/MCF7-PBX1-ChIP-Seq(GSE28007)	GSCTGTCACTCA	3.61E+00
23	FOXA1:AR(Forkhead,NR)/LNCAP-AR-ChIP-Seq(GSE27824)	AGTAAACAAAAAAGAACAND	3.56E+00
24	DMRT6(DM)/Testis-DMRT6-ChIP-Seq(GSE60440)	YDGHTACAWTGTADC	3.51E+00
25	NeuroD1(bHLH)/Islet-NeuroD1-ChIP-Seq(GSE30298)	GCCATCTGTT	3.48E+00
26	Tgif1(Homeobox)/mES-Tgif1-ChIP-Seq(GSE55404)	YTGWCADY	3.41E+00
27	ZNF519(Zf)/HEK293-ZNF519.GFP-ChIP-Seq(GSE58341)	GAGSCCGAGC	3.38E+00
28	FoxL2(Forkhead)/Ovary-FoxL2-ChIP-Seq(GSE60858)	WWTRTAAACAVG	3.36E+00
29	Chop(bZIP)/MEF-Chop-ChIP-Seq(GSE35681)	ATTGCATCAT	3.36E+00
30	Six1(Homeobox)/Myoblast-Six1-ChIP-Chip(GSE20150)	GKVTCADRTTWC	3.35E+00

* Significance P-value < 0.0001 estimated by Homer v4.11. The motifs shown in Figure 5H are highlighted yellow.

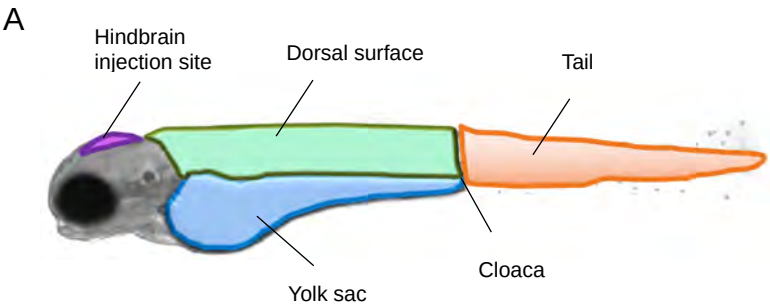
A
Hindbrain injection site
Dorsal surface
Tail
Cloaca
Yolk sac

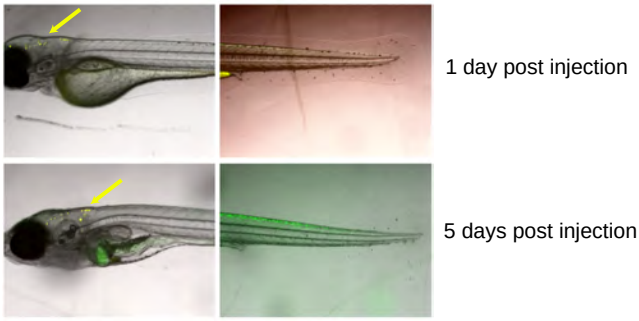
B
1 day post injection
5 days post injection

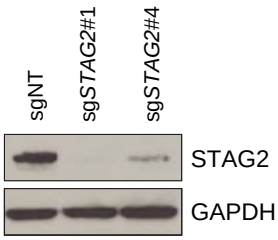
C
sgNT
sgSTAG2#1
sgSTAG2#4
STAG2
GAPDH

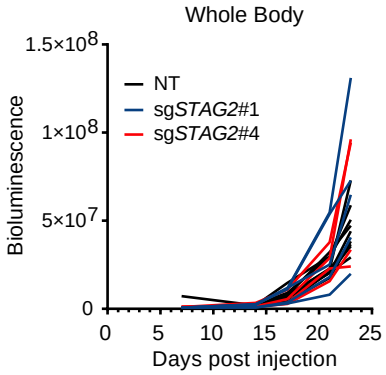
D
Whole Body
Bioluminescence
1.5×10^8
1×10^8
5×10^7
0
NT
sgSTAG2#1
sgSTAG2#4
0 5 10 15 20 25
Days post injection

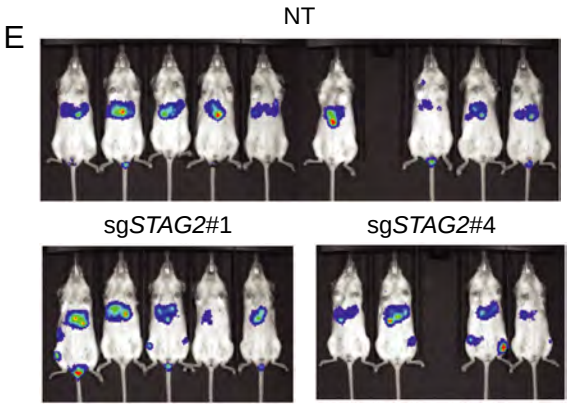
E
NT
sgSTAG2#1
sgSTAG2#4

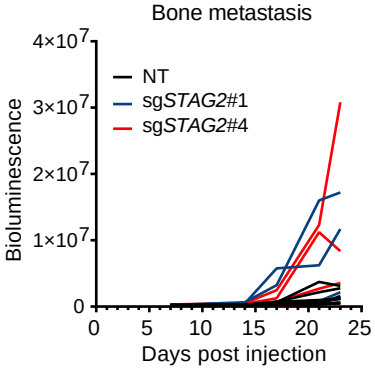
F
Bone metastasis
Bioluminescence
4×10^7
3×10^7
2×10^7
1×10^7
0
NT
sgSTAG2#1
sgSTAG2#4
0 5 10 15 20 25
Days post injection

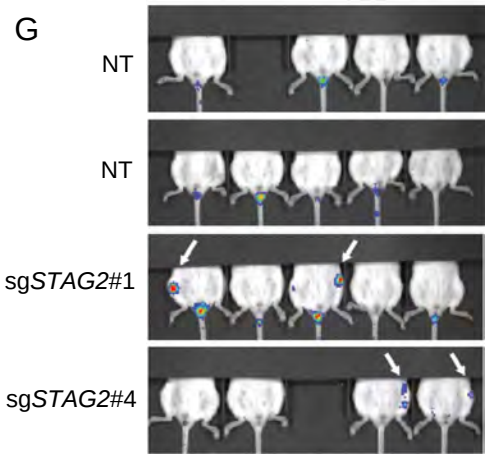
G
NT
NT
sgSTAG2#1
sgSTAG2#4

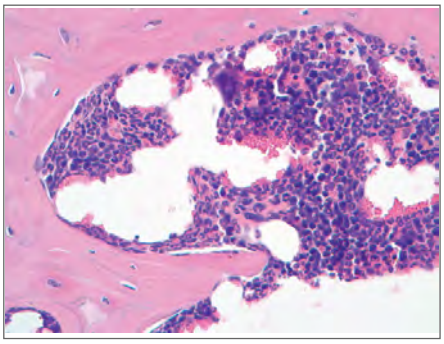
H

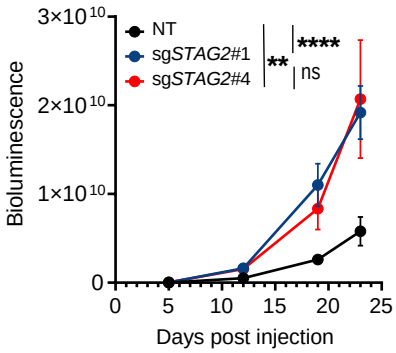
I
Bioluminescence
3×10^10
2×10^10
1×10^10
0
NT
sgSTAG2#1
sgSTAG2#4
**
****
ns
0 5 10 15 20 25
Days post injection

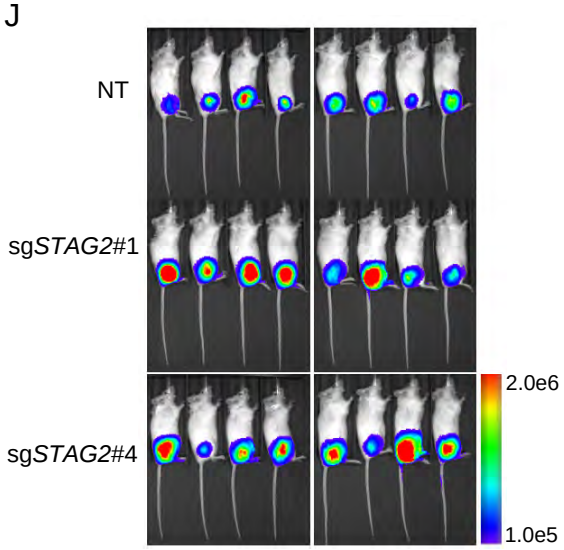
J
NT
sgSTAG2#1
sgSTAG2#4
2.0e6
1.0e5

K

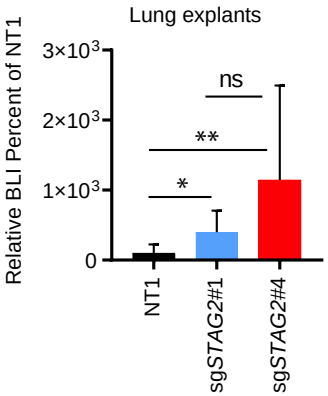
Lung explants
Relative BLI Percent of NT1
3×10^3
2×10^3
1×10^3
0
ns
**
*
NT1
sgSTAG2#1
sgSTAG2#4

L

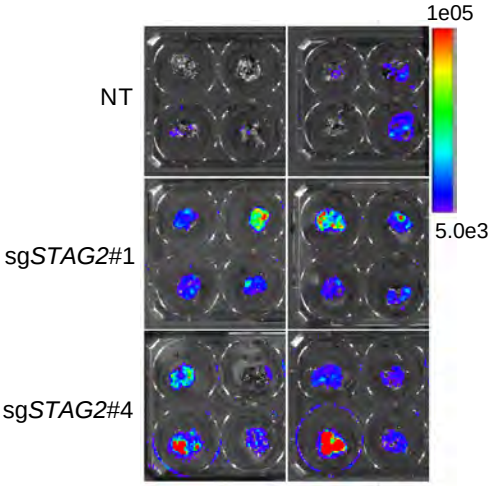
1e05
5.0e3
NT
sgSTAG2#1
sgSTAG2#4

M

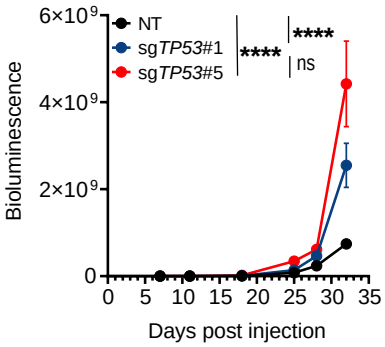
Bioluminescence
6×10^9
4×10^9
2×10^9
0
NT
sgTP53#1
sgTP53#5
****
****
ns
0 5 10 15 20 25 30 35
Days post injection

N

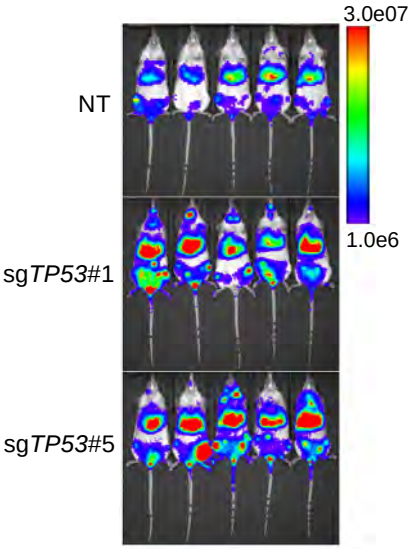
3.0e07
1.0e6
NT
sgTP53#1
sgTP53#5

O

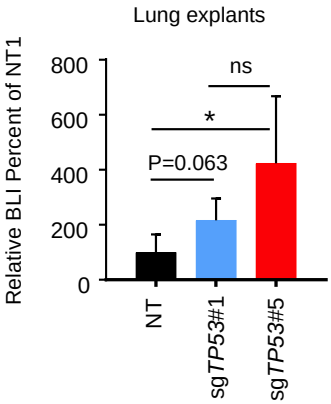
Lung explants
Relative BLI Percent of NT1
800
600
400
200
0
ns
*
P=0.063
NT
sgTP53#1
sgTP53#5

P

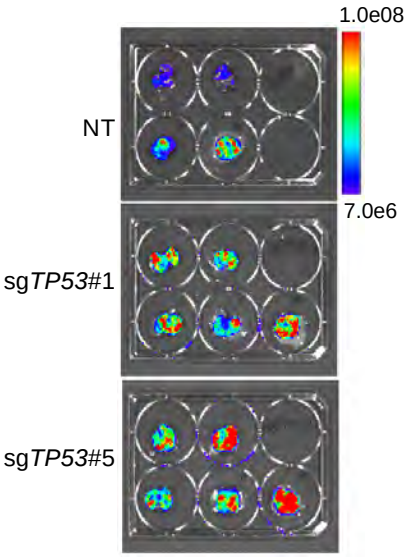
1.0e08
7.0e6
NT
sgTP53#1
sgTP53#5

Figure S6. Depletion of *STAG2* enhances the migration and metastatic potential of Ewing sarcoma cells, related to Figure 6.

(A) Diagram describing the anatomical locations used for injection (hindbrain region) and the assessment of migration (dorsal surface, tail and yolk sac).

(B) Larvae were injected with fluorescent microspheres (~10 microns in size, yellow dots) into the hind brain ventricles 2 days post fertilization (dpf). Larvae were monitored for passive microsphere migration into the dorsal surface, yolk sac and tail. Images show representative zebrafish at days 1 (top) and 5 (bottom) post injection

(C) Western blot showing the levels of *STAG2* in polyclonal control and *STAG2* KO TC71 cells. *GAPDH* was used as a loading control.

(D) Polyclonal control and *STAG2* KO TC71 cells were injected via tail vein of recipient NSG mice. Quantification of bioluminescence signal collected for whole body is shown. Each line of the spaghetti plot represents a single mouse. N = 8 for NT and N = 4 for sg*STAG2*#1 and sg*STAG2*#4.

(E) Bioluminescence images of mice described in Figure S6D are shown.

(F) Polyclonal control and *STAG2* KO TC71 cells were injected via tail vein of recipient NSG mice. Quantification of bioluminescence signal collected for lower extremities after blocking upper abdominal cavity is shown. Each line of the spaghetti plot represents a single mouse. N = 8 for NT and N = 4 for sg*STAG2*#1 and sg*STAG2*#4.

(G) Bioluminescence images of mice described in Figure S6F are shown. White arrows indicate marrow infiltration of Ewing sarcoma cells.

(H) A representative H&E stained bone marrow of a mouse injected with *STAG2* KO cells is shown.

(I) Clonally selected control (NT) and *STAG2* KO A673 cells were injected into the lower leg intramuscular space of recipient NSG mice. Quantification of bioluminescence signal collected for whole body is shown. Line graph represents mean $\pm$ SEM, N = 8 per group. Two-way ANOVA, **** $P < 0.0001$, ** $P < 0.01$, ns = not significant.

(J) Bioluminescence images of lungs described in Figure S6I are shown.

(K) Clonally selected control and *STAG2* KO A673 cells were injected into the lower leg intramuscular space of recipient NSG mice. Lungs were extracted from mice at the conclusion of the study and imaged ex vivo. Quantification of bioluminescence signal for lungs normalized to NT signal is shown. Bar graphs represents mean ± standard deviation, N = 8 per group. Mann-Whitney non-parametric t-test, ** $P < 0.001$, * $P < 0.05$, ns = not significant.

(L) Bioluminescence images of lung explants described in Figure S6K are shown.

(M) Polyclonal control and *TP53* KO TC32 cells were injected via tail vein of recipient NSG mice. Quantification of bioluminescence signal collected for whole body is shown. Line graph represents mean ± SEM, N = 5 per group. Two-way ANOVA, **** $P < 0.0001$, ns = not significant.

(N) Bioluminescence images of mice described in Figure S6M are shown.

(O) Lungs were extracted from mice described in Figures S6M and S6N at the conclusion of the study and imaged ex vivo. Quantification of bioluminescence signal for lungs normalized to NT signal is shown (left). Bar graphs represents mean ± SD, N = 8 per group. Mann-Whitney non-parametric t-test, * $P < 0.05$, ns = not significant. Bioluminescence images of lungs described are shown (right).

(P) Bioluminescence images of lung explants described in Figure S6O are shown.

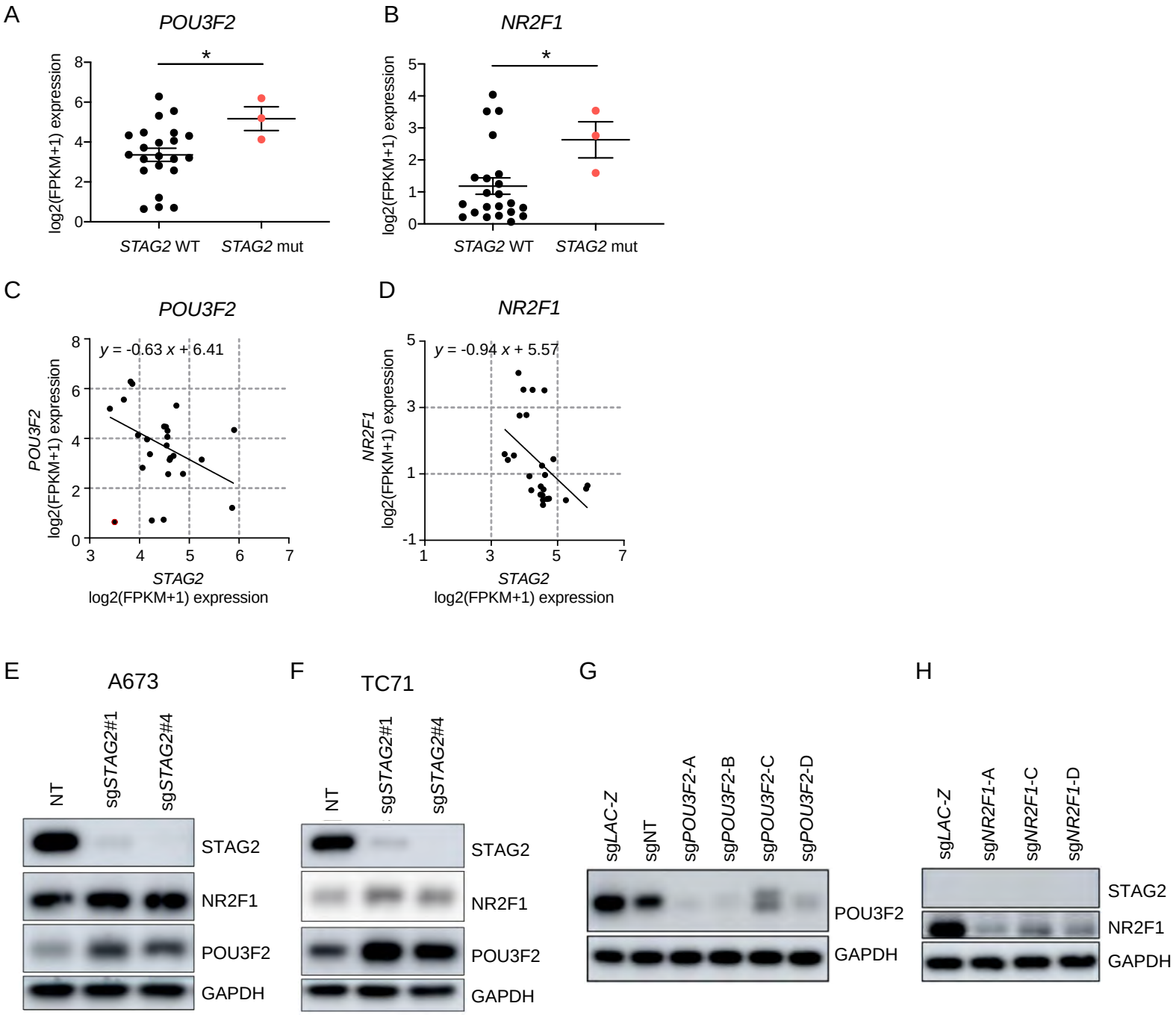
A
POU3F2
log2(FPKM+1) expression
STAG2 WT
STAG2 mut
B
NR2F1
log2(FPKM+1) expression
STAG2 WT
STAG2 mut
C
POU3F2
y = -0.63 x + 6.41
POU3F2 log2(FPKM+1) expression
STAG2 log2(FPKM+1) expression
D
NR2F1
y = -0.94 x + 5.57
NR2F1 log2(FPKM+1) expression
STAG2 log2(FPKM+1) expression
E
A673
NT
sgSTAG2#1
sgSTAG2#4
STAG2
NR2F1
POU3F2
GAPDH
F
TC71
NT
sgSTAG2#1
sgSTAG2#4
STAG2
NR2F1
POU3F2
GAPDH
G
sgLAC-Z
sgNT
sgPOU3F2-A
sgPOU3F2-B
sgPOU3F2-C
sgPOU3F2-D
POU3F2
GAPDH
H
sgLAC-Z
sgNR2F1-A
sgNR2F1-C
sgNR2F1-D
STAG2
NR2F1
GAPDH

Figure S7. The neurodevelopmental transcription factor *POU3F2* modulates the metastatic potential of *STAG2* KO Ewing sarcoma cells, related to Figure 7.

(A)-(B) mRNA log2(FPKM+1) expression level of (A) *POU3F2* and (B) *NR2F1* in 3 *STAG2* mutant and 22 *STAG2* WT tumors from Crompton et al. (2014). Mann-Whitney non-parametric t-test, * $P < 0.05$.

(C)-(D) Linear regression model fit for the log2(FPKM+1) expression of (C) *POU3F2* and (D) *NR2F1* vs. the log2(FPKM+1) *STAG2* expression in Ewing tumors from Crompton et al. (2014) is shown. Goodness-of-fit and the Kolmogorov-Smirnov normality test for residuals, ** $P < 0.01$, * $P < 0.05$.

(E) Polyclonal *STAG2* KO A673 cells were generated using CRISPR/Cas9 mediated genome editing. The expression levels of *STAG2*, *POU3F2* and *NR2F1* in control (NT) and *STAG2* KO cells were assessed by western blotting. GAPDH was used as a loading control.

(F) Polyclonal *STAG2* KO TC71 cells were generated using CRISPR/Cas9 mediated genome editing. The expression levels of *STAG2*, *POU3F2* and *NR2F1* in control (NT) and *STAG2* KO cells were assessed by western blotting. GAPDH was used as a loading control.

(G) Clonally selected *STAG2* KO A673 cells were used to generate polyclonal *POU3F2* KO cells using CRISPR/Cas9 mediated genome editing. The expression levels of *POU3F2* in control (*LAC-Z* and NT) and *POU3F2* KO cells were assessed by western blotting. GAPDH was used as a loading control. sg*LAC-Z* and sg*POU3F2*-A were used for xenograft studies described in Figures 7G-J.

(H) Clonally selected *STAG2* KO A673 cells were used to generate polyclonal *NR2F1* KO cells using CRISPR/Cas9 mediated genome editing. The expression levels of *NR2F1* and *STAG2* in control (sg*LAC-Z*) and KO cells were assessed by western blotting. GAPDH was used as a loading control. sg*LAC-Z* and sg*NR2F1*-A were used for xenograft studies described in Figures 7G-J.